J|A|C|S
ARTICLES
Published on Web 08/02/2006

Electrochemical, Spectroelectrochemical, and Molecular Quadratic and Cubic Nonlinear Optical Properties of Alkynylruthenium Dendrimers[1]

Marie P. Cifuentes,[†] Clem E. Powell,[†] Joseph P. Morrall,[†,‡] Andrew M. McDonagh,[†] Nigel T. Lucas,[†] Mark G. Humphrey,*[,†] Marek Samoc,[‡] Stephan Houbrechts,[§] Inge Asselberghs,[§] Koen Clays,[§] André Persoons,[§] and Takashi Isoshima[#]

Contribution from the Department of Chemistry and Laser Physics Centre, Research School of Physical Sciences and Engineering, Australian National University, Canberra ACT 0200, Australia, Department of Chemistry, University of Leuven, Celestijnenlaan 200D, B-3001 Leuven, Belgium, and Local Spatio-Temporal Functions Laboratory, Frontier Research System, RIKEN (The Institute of Physical and Chemical Research), 2-1 Hirosawa, Wako, Saitama 351-0198, Japan

Received April 2, 2006; E-mail: Mark.Humphrey@anu.edu.au

Abstract: A combination of cyclic voltammetry (CV), UV−vis−NIR spectroscopy and spectroelectrochemistry, hyper-Rayleigh scattering (HRS) [including depolarization studies], Z-scan and degenerate four-wave mixing (DFWM) [including studies employing an optically transparent thin-layer electrochemical (OTTLE) cell to effect electrochemical switching of nonlinearity], pump−probe, and electroabsorption (EA) measurements have been used to comprehensively investigate the electronic, linear optical, and nonlinear optical (NLO) properties of nanoscopic π-delocalizable electron-rich alkynylruthenium dendrimers, their precursor dendrons, and their linear analogues. CV, UV−vis−NIR spectroscopy, and UV−vis−NIR spectroelectrochemistry reveal that the reversible metal-centered oxidation processes in these complexes are accompanied by strong linear optical changes, "switching on" low-energy absorption bands, the frequency of which is tunable by ligand replacement. HRS studies at 1064 nm employing nanosecond pulses reveal large nonlinearities for these formally octupolar dendrimers; depolarization measurements are consistent with lack of coplanarity upon π-framework extension through the metal. EA studies at 350−800 nm in a poly(methyl methacrylate) matrix are consistent with the important transitions having a charge-transfer exciton character that increases markedly on introduction of peripheral polarizing substituent. Time-resolved pump−probe studies employing 55 ps, 527 nm pulses reveal absorption saturation, the longest excited-state lifetime being observed for the dendrimer. Z-scan studies at 800 nm employing femtosecond pulses reveal strong two-photon absorption that increases significantly on progression from linear complex to zero- and then first-generation dendrimer with no loss of optical transparency. Both refractive and absorptive nonlinearity for selected alkynylruthenium dendrimers have been reversibly "switched" by employing the Z-scan technique at 800 and 1180 nm and 100−150 fs pulses, together with a specially modified OTTLE cell, complementary femtosecond time-resolved DFWM and transient absorption studies at 800 nm suggesting that the NLO effects originate in picosecond time scale processes.

Introduction

Dendrimers are monodisperse hyperbranched molecules that have attracted significant interest recently as novel materials with potential applications in *inter alia* medical diagnostics, molecular recognition, catalysis, and photoactive device engineering.[2−5] The first examples of dendrimers were purely organic in composition, and organic dendrimers continue to dominate the field, but inorganic[6−13] and, more recently, organometallic dendrimers[14−39] have been the focus of interest

[†] Department of Chemistry, Australian National University.
[‡] Laser Physics Centre, Research School of Physical Sciences and Engineering, Australian National University.
[§] University of Leuven.
[#] RIKEN.

(1) Organometallic Complexes for Nonlinear Optics. Part 35. For part 34, see: Powell, C. E.; Morrall, J. P. L.; Ward, S. A.; Cifuentes, M. P.; Notaras, E. G. A.; Samoc, M.; Humphrey, M. G. *J. Am. Chem. Soc.* **2004**, *126*, 12234.
(2) Put, E. J. H.; Clays, K.; Persoons, A.; Biemans, H. A. M.; Luijkx, C. P. M.; Meijer, E. W. *Chem. Phys. Lett.* **1996**, *260*, 136.
(3) Zeng, F. W.; Zimmerman, S. C. *Chem. Rev.* **1997**, *97*, 1681.
(4) Archut, A.; Vögtle, F. *Chem. Soc. Rev.* **1998**, *27*, 233.
(5) Fischer, M.; Vögtle, F. *Angew. Chem., Int. Ed.* **1999**, *38*, 885.
(6) McClenaghan, N. D.; Passalacqua, R.; Loiseau, F.; Campagna, S.; Verheyde, B.; Hameurlaine, A.; Dehaen, W. *J. Am. Chem. Soc.* **2003**, *125*, 5366.
(7) Hong, Y.-R.; Gorman, C. B. *J. Org. Chem.* **2003**, *68*, 9019.
(8) Ceroni, P.; Vicinelli, V.; Maestri, M.; Balzani, V.; Lee, S.-K.; van Heyst, J.; Gorka, M.; Vögtle, F. *J. Organomet. Chem.* **2004**, *689*, 4375.
(9) Krishna, T. R.; Jayaraman, N. *Tetrahedron* **2004**, *60*, 10325.
(10) Saudan, C.; Balzani, V.; Gorka, M.; Lee, S.-K.; van Heyst, J.; Maestri, M.; Ceroni, P.; Vicinelli, V.; Vögtle, F. *Chem. Eur. J.* **2004**, *10*, 899.
(11) Constable, E. C.; Housecroft, C. E.; Neuburger, M.; Schaffner, S.; Scherer, L. J. *Dalton Trans.* **2004**, 2635.
(12) Imaoka, T.; Tanaka, R.; Arimoto, S.; Sakai, M.; Fujii, M.; Yamamoto, K. *J. Am. Chem. Soc.* **2005**, *127*, 13896.
(13) Puntoriero, F.; Serroni, S.; Galletta, M.; Juris, A.; Licciardello, A.; Chiorboli, C.; Campagna, S.; Scandola, F. *Chem. Phys. Chem.* **2005**, *6*, 129.

because the metal may imbue the dendritic material with specific optical, electronic, magnetic, catalytic, and other properties; indeed, hybrid inorganic−organometallic dendrimers have recently been reported.[40] The great majority of metal-containing dendrimers are peripherally metallated organic dendrimers;[41−66] organometallic dendrimers with transition metals in every generation are comparatively rare,[26,34,67−76] the scarcity having been suggested to derive from the intrinsically lower stability of most organometallic complexes compared to organic compounds, coupled to the need to build up the dendrimer by successive organometallic reactions.[72]

We have been examining the nonlinear optical (NLO) properties of alkynylmetal complexes and have noted an enhancement of NLO response upon increasing the metal valence electron count in linear (rodlike) alkynylmetal complexes.[77−81] NLO materials with a dendritic construction may have enhanced nonlinearities, coupled to favorable transparency and processing characteristics, because the 1,3,5-trisubstituted benzene branching points in arylalkynyl dendrimers may permit extensive π-delocalization without appreciable red-shift of the important linear optical absorption band(s). Electron-rich π-delocalizable organometallic dendrimers are therefore of considerable interest, but the vast majority of π-delocalizable organometallic dendrimers have employed 16-electron metal centers. We recently reported synthetic procedures leading to bis(diphosphine)ruthenium-containing arylalkynyl dendrimers containing 18-electron metal centers, including systematically varied dendrimer examples peripherally functionalized by electron-donating (NEt_2) or electron-withdrawing (NO_2) substituents.[82] We report herein the electrochemical, linear optical, and spectroelectrochemical properties of these electron-rich alkynylruthenium dendrimers, their quadratic NLO properties as determined from hyper-Rayleigh scattering (HRS) at 1064 nm, their cubic NLO properties as determined from femtosecond Z-scan at 800, 1180, and 1300 nm and degenerate four-wave mixing (DFWM) studies at 800 nm, their third-order NLO susceptibilities $\chi^{(3)}$ determined by electroabsorption (EA) spectroscopy in resonance at ca. 450 nm, electrochemical switching of both refractive and absorptive molecular cubic nonlinearity, picosecond pump−probe studies at 527 nm to determine

(14) Hearshaw, M. A.; Moss, J. R. *Chem. Commun.* **1999**, 1.
(15) Stoddart, F. J.; Welton, T. *Polyhedron* **1999**, *18*, 3575.
(16) Cuadrado, I.; Morán, M.; Casado, C. M.; Alonso, B.; Losada, J. *Coord. Chem. Rev.* **1999**, *193*−*5*, 395.
(17) Astruc, D.; Blais, J.-C.; Cloutet, E.; Djakovitch, L.; Rigaut, S.; Ruiz, J.; Sartor, V.; Valério, C. In *Topics in Current Chemistry*; Vögtle, F., Ed.; Springer: Berlin, Germany, 2000; Vol. 210, p 229.
(18) Juris, A.; Venturi, M.; Ceroni, P.; Balzani, V.; Campagna, S.; Serroni, S. *Collect. Czech. Chem. Commun.* **2001**, *66*, 1.
(19) van Manen, H.-J.; van Veggel, F. C. J. M.; Reinhoudt, D. N. In *Topics in Current Chemistry*; Vögtle, F., Schalley, C. A., Eds.; Springer: Berlin, Germany, 2001; Vol. 217, p 121.
(20) Kreiter, R.; Kleij, A. W.; Klein Gebbink, R. J. M.; van Koten, G. In *Topics in Current Chemistry*; Vögtle, F., Schalley, C. A., Eds.; Springer: Berlin, Germany, 2001; Vol. 217, p 163.
(21) Astruc, D. *Pure Appl. Chem.* **2003**, *75*, 461.
(22) Bourrier, O.; Kakkar, A. K. *J. Mater. Chem.* **2003**, *13*, 1306.
(23) Sengupta, S. *Tetrahedron Lett.* **2003**, *44*, 7281.
(24) Poniatowska, E.; Salamończyk, G. M. *Tetrahedron Lett.* **2003**, *44*, 4315.
(25) Angurell, I.; Muller, G.; Rocamora, M.; Rossell, O.; Seco, M. *Dalton Trans.* **2003**, 1194.
(26) Onitsuka, K.; Shimizu, A.; Takahashi, S. *Chem. Commun.* **2003**, 280.
(27) Dijstra, H. P.; Kruithof, C. A.; Ronde, N.; van de Coevering, R.; Ramón, D. J.; van Klink, G. P. M.; van Koten, G. *J. Org. Chem.* **2003**, *68*, 675.
(28) Albinati, A.; Leoni, P.; Marchetti, L.; Rizzato, S. *Angew. Chem., Int. Ed.* **2003**, *42*, 5990.
(29) Angurell, I.; Muller, G.; Rocamora, M.; Rossell, O.; Seco, M. *Dalton Trans.* **2004**, 2450.
(30) Astruc, D. *J. Organomet. Chem.* **2004**, *689*, 4332.
(31) Busetto, L.; Cassani, M. C.; van Leeuwen, P. W. N. M.; Mazzoni, R. *Dalton Trans.* **2004**, 2767.
(32) Diaz, C.; Barbosa, M.; Godoy, Z. *Polyhedron* **2004**, *23*, 1027.
(33) Frampton, M. J.; Namdas, E. B.; Lo, S.-C.; Burn, P. L.; Samuel, I. D. W. *J. Mater. Chem.* **2004**, *14*, 2881.
(34) Chase, P. A.; Klein Gebbinck, R. J. M.; van Koten, G. *J. Organomet. Chem.* **2004**, *689*, 4016.
(35) Onitsuka, K.; Fujimoto, M.; Kitajima, H.; Ohshiro, N.; Takei, F.; Takahashi, S. *Chem. Eur. J.* **2004**, *10*, 6433.
(36) Caminade, A.-M.; Majoral, J.-P. *Coord. Chem. Rev.* **2005**, *249*, 1917.
(37) Turrin, C.-O.; Donnadieu, B.; Caminade, A.-M.; Majoral, J.-P. *Z. Anorg. Allg. Chem.* **2005**, *631*, 2881.
(38) Angurall, I.; Rossell, O.; Seco, M.; Ruiz, E. *Organometallics* **2005**, *24*, 6365.
(39) Ornelas, C.; Vertlib, V.; Rodrigues, J.; Rissanen, K. *Eur. J. Inorg. Chem.* **2006**, *1*, 47.
(40) Méry, D.; Plault, L.; Ornelas, C.; Ruiz, J.; Nlate, S.; Astruc, D.; Blais, J.-C.; Rodrigues, J.; Cordier, S.; Kirakci, K.; Perrin, C. *Inorg. Chem.* **2006**, *45*, 1156.
(41) Liao, Y.-H.; Moss, J. R. *J. Chem. Soc., Chem. Commun.* **1993**, 1774.
(42) Alonso, B.; Cuadrado, I.; Morán, M.; Losada, J. *J. Chem. Soc., Chem. Commun.* **1994**, 2575.
(43) Alonso, B.; Morán, M.; Casado, C. M.; Lobete, F.; Losada, J.; Cuadrado, I. *Chem. Mater.* **1995**, *7*, 1440.
(44) Liao, Y.-H.; Moss, J. R. *Organometallics* **1995**, *14*, 2130.
(45) Cuadrado, I.; Morán, M.; Moya, A.; Casado, C. M.; Barranco, M.; Alonso, B. *Inorg. Chim. Acta* **1995**, *251*, 5.
(46) Lobete, F.; Cuadrado, I.; Casado, C. M.; Alonso, B.; Morán, M.; Losada, J. *J. Organomet. Chem.* **1996**, *509*, 109.
(47) Liao, Y.-H.; Moss, J. R. *Organometallics* **1996**, *15*, 4307.
(48) Shu, C.-F.; Shen, H.-M. *J. Mater. Chem.* **1997**, *7*, 47.
(49) Losada, J.; Cuadrado, I.; Morán, M.; Casado, C. M.; Alonso, B.; Barranco, M. A. *Anal. Chim. Acta* **1997**, *338*, 191.
(50) Cuadrado, I.; Casado, C. M.; Alonso, B.; Morán, M.; Losada, J.; Belsky, V. *J. Am. Chem. Soc.* **1997**, *119*, 7613.
(51) Kriesel, J. W.; König, S.; Freitas, M. A.; Marshall, A. G.; Leary, J. A.; Tilley, T. D. *J. Am. Chem. Soc.* **1998**, *120*, 12207.
(52) Gossage, R. A.; Jastrzebski, J. J. B. H.; van Armeijde, J.; Mulders, S. J. E.; Brouwer, A. J.; Liskamp, R. M. J.; van Koten, G. *Tetrahedron Lett.* **1999**, *40*, 1413.
(53) Naidoo, K. J.; Hughes, S. J.; Moss, J. R. *Macromolecules* **1999**, *32*, 331.
(54) van Koten, G.; Jastrzebski, J. J. B. H. *J. Mol. Catal. A: Chem.* **1999**, *146*, 317.
(55) Albrecht, M.; Gossage, R. A.; Lutz, M.; Spek, A. L.; van Koten, G. *Chem. Eur. J.* **2000**, *6*, 1431.
(56) Vlcek, A., Jr. *Chemtracts*−*Inorg. Chem.* **2000**, *13*, 810.
(57) Casado, C. M.; González, B.; Cuadrado, I.; Alonso, B.; Morán, M.; Losada, J. *Angew. Chem., Int. Ed.* **2000**, *39*, 2135.
(58) Mavunkal, I. J.; Moss, J. R.; Bacsa, J. *J. Organomet. Chem.* **2000**, *593-4*, 361.
(59) Valentini, M.; Pregosin, P. S.; Rüegger, H. *Organometallics* **2000**, *19*, 2551.
(60) Hovestad, N. J.; Ford, A.; Jastrzebski, J. J. B. H.; van Koten, G. *J. Org. Chem.* **2000**, *65*, 6338.
(61) Hurley, A. L.; Mohler, D. L. *Org. Lett.* **2000**, *2*, 2745.
(62) Nlate, A. L.; Ruiz, J.; Sartor, V.; Navarro, R.; Blais, J.-C.; Astruc, D. *Chem. Eur. J.* **2000**, *6*, 2544.
(63) Turrin, C.-O.; Chiffre, J.; Daran, J.-C.; de Montauzon, D.; Caminade, A.-M.; Manoury, E.; Balavoine, G.; Majoral, J.-P. *Tetrahedron* **2001**, *57*, 2521.
(64) Hurst, S.; Cifuentes, M. P.; Humphrey, M. G. *Organometallics* **2002**, *21*, 2353.
(65) van de Coevering, R.; Kuil, M.; Klein Gebbink, R. J. M.; van Koten, G. *Chem. Commun.* **2002**, 1636.
(66) Dijkstra, H. P.; Kruithof, C. A.; Ronde, N.; van de Coevering, R.; Ramon, D. J.; Vogt, D.; van Klink, G. P. M.; van Koten, G. *J. Org. Chem.* **2003**, *68*, 675.
(67) Ohshiro, N.; Takei, F.; Onitsuka, K.; Takahashi, S. *Chem. Lett.* **1996**, 871.
(68) Achar, S.; Vittal, J. J.; Puddephatt, R. J. *Organometallics* **1996**, *15*, 43.
(69) Achar, S.; Immoos, C. E.; Hill, M. G.; Catalano, V. J. *Inorg Chem.* **1997**, *36*, 2314.
(70) Leininger, S.; Stang, P. J.; Huang, S. *Organometallics* **1998**, *17*, 3981.
(71) Ohshiro, N.; Takei, F.; Onitsuka, K.; Takahashi, S. *J. Organomet. Chem.* **1998**, *569*, 195.
(72) Onitsuka, K.; Fujimoto, M.; Ohshiro, N.; Takahashi, S. *Angew. Chem., Int. Ed.* **1999**, *38*, 689.
(73) McDonagh, A. M.; Humphrey, M. G.; Samoc, M.; Luther-Davies, B. *Organometallics* **1999**, *18*, 5195.
(74) Turrin, C.-O.; Chiffre, J.; de Montauzon, D.; Daran, J.-C.; Caminade, A.-M.; Manoury, E.; Balavoine, G.; Majoral, J.-P. *Macromolecules* **2000**, *33*, 7328.
(75) Onitsuka, K.; Iuchi, A.; Fujimoto, M.; Takahashi, S. *Chem. Commun.* **2001**, 741.
(76) Onitsuka, K.; Takahashi, S. *Top. Curr. Chem.* **2003**, *228*, 39.
(77) Whittall, I. R.; Humphrey, M. G.; Houbrechts, S.; Persoons, A.; Hockless, D. C. R. *Organometallics* **1996**, *15*, 5738.
(78) Whittall, I. R.; Cifuentes, M. P.; Humphrey, M. G.; Luther-Davies, B.; Samoc, M.; Houbrechts, S.; Persoons, A.; Heath, G. A.; Bogsanyi, D. *Organometallics* **1997**, *16*, 2631.
(79) Whittall, I. R.; Cifuentes, M. P.; Humphrey, M. G.; Luther-Davies, B.; Samoc, M.; Houbrechts, S.; Persoons, A.; Heath, G. A.; Hockless, D. C. R. *J. Organomet. Chem.* **1997**, *549*, 127.
(80) Powell, C. E.; Humphrey, M. G. *Coord. Chem. Rev.* **2004**, *248*, 725.
(81) Cifuentes, M. P.; Humphrey, M. G. *J. Organomet. Chem.* **2004**, *689*, 3968.
(82) McDonagh, A. M.; Powell, C. E.; Morrall, J. P.; Cifuentes, M. P.; Humphrey, M. G. *Organometallics* **2003**, *22*, 1402.

absorption saturation properties, and an assessment of the effect of "dimensional evolution" [in progressing from linear (1D) molecules to 2D octupolar and dendritic molecules] upon these important properties; some of these results for selected complexes lacking peripheral substituents have been reported in a preliminary form.[73,83−85]

Experimental Section

Synthetic Procedures. The complexes *trans*-[Ru(C≡CC_6H_4-4-C≡CPh)X(dppe)$_2$] [X = Cl (**7a**),[86] C≡CPh (**7b**), 4-C≡$CC_6H_4NO_2$ (**7c**), 4-C≡$CC_6H_4NEt_2$ (**7d**)], 1-(Me_3SiC≡C)C_6H_3-3,5-{4-C≡CC_6H_4C≡C-*trans*-[RuX(dppe)$_2$]}$_2$ [X = Cl (**2a**), C≡CPh (**2b**), 4-C≡$CC_6H_4NO_2$ (**2c**), 4-C≡$CC_6H_4NEt_2$ (**2d**)], 1-(HC≡C)C_6H_3-3,5-{4-C≡CC_6H_4C≡C-*trans*-[RuX(dppe)$_2$]}$_2$ [X = C≡CPh (**3a**), 4-C≡$CC_6H_4NO_2$ (**3b**)], 1,3,5-C_6H_3{4-C≡CC_6H_4C≡C-*trans*-[RuX(dppe)$_2$]}$_2$ [X = Cl (**5a**), C≡CPh (**5b**), 4-C≡$CC_6H_4NO_2$ (**5c**), 4-C≡$CC_6H_4NEt_2$ (**5d**)], 1,3,5-C_6H_3{4-C≡CC_6H_4C≡C-*trans*-[RuCl(dppm)$_2$]}$_3$ (**8**), [1,3,5-C_6H_3{4-C≡CC_6H_4CH=C-*trans*-RuCl(L_2)$_2$}$_3$][PF_6]$_3$ [L_2 = dppm (**9a**), dppe (**9b**)], and 1,3,5-C_6H_3(4-C≡CC_6H_4C≡C-*trans*-[Ru(dppe)$_2$]C≡C-3,5-C_6H_3{4-C≡CC_6H_4C≡C-*trans*-[RuX(dppe)$_2$]}$_2$)$_3$ [X = C≡CPh (**6a**), 4-C≡$CC_6H_4NO_2$ (**6b**)], and the alkynes 1,3,5-C_6H_3(4-C≡CC_6H_4C≡CSiMe_3)$_3$ (**4**) and 1-Me_3-SiC≡C-3,5-(4-XC_6H_4C≡C)$_2C_6H_3$ [X = Br (**1a**), I (**1b**), C≡CH (**1c**)][82] were prepared according to previously reported procedures.

Linear Optical, Electrochemical, and Spectroelectrochemical Studies. UV−vis spectra were recorded as tetrahydrofuran (THF) solutions in 1 cm cells using a Cary 5 spectrophotometer. Cyclic voltammetric measurements were recorded using a MacLab 400 interface and MacLab potentiostat from ADInstruments (using Pt disk working, Pt auxiliary, and Ag−AgCl reference mini-electrodes from Cypress Systems). Scan rates were typically 100 mV s^{-1}. Electrochemical solutions contained 0.1 M (NBu^n_4)PF_6 and ca. 10^{-3} M complex in CH_2Cl_2. Solutions were purged and maintained under an atmosphere of argon. All values are referenced to an internal ferrocene/ferrocenium couple (E^0 at 0.56 V). Spectroelectrochemical data were recorded on a Cary 5 spectrophotometer (220−2500 nm, 45 000−4000 cm^{-1}) in CH_2Cl_2. Solution spectra of the oxidized species at 253 K were obtained by electrogeneration (Thompson 401E potentiostat) at a Pt gauze working electrode within a cryostatted optically transparent thin-layer electrochemical (OTTLE) cell, path length 0.5 mm, mounted within the spectrophotometer.[87] The electrogeneration potential was ca. 300 mV beyond $E_{1/2}$ for each couple, to ensure complete electrolysis. The efficiency and reversibility of each step were tested by applying a sufficiently negative potential to reduce the product; stable isosbestic points were observed in the spectral progressions for all the transformations reported herein.

Hyper-Rayleigh Scattering Measurements. A beam from a Nd:YAG laser [Q-switched Nd:YAG Quanta Ray GCR130-10, 1064 nm (9400 cm^{-1}), 8 ns pulses, 10 Hz] was focused into a cylindrical cell (14 mL) containing the sample. The intensity of the incident beam was varied by rotation of a half-wave plate placed between crossed polarizers. Part of the laser pulse was sampled by a photodiode to measure the vertically polarized incident fundamental light intensity. The frequency-doubled light was collected by an efficient condenser system and detected by a photomultiplier. The harmonic scattering and linear scattering were distinguished by appropriate filters; gated integrators were used to obtain intensities of the incident and harmonic scattered light.[88−90] All compounds were additionally checked for fluorescence using a commercial spectrometer and exciting at 355 nm (28 200 cm^{-1}) and 532 nm (18 800 cm^{-1}); no emission was detected in the range 350−700 nm (28 600−14 300 cm^{-1}) for any complex reported herein. All measurements were performed in THF using *p*-nitroaniline ($\beta = 21.4 \times 10^{-30}$ esu) as a reference. To perform depolarization measurements,[91−94] the condensor system was omitted and a rotating analyzing polarizer was placed in front of the photomultiplier.

Z-Scan Measurements. Measurements at 800 nm (12 500 cm^{-1}) used 100 fs pulses from a system consisting of a Coherent Mira Ti-sapphire laser pumped with a Coherent Verdi continuous-wave pump and a Ti-sapphire regenerative amplifier pumped with a frequency-doubled Q-switched pulsed Nd:YAG laser (Spectra Physics GCR) at 30 Hz and employing chirped pulse amplification. THF solutions were examined in a 0.1 cm path length cell. The closed-aperture and open-aperture Z-scans were recorded at a few concentrations of each compound, and the real and imaginary parts of the nonlinear phase shift were determined by numerical fitting using equations given in ref 95. The real and imaginary parts of the hyperpolarizability of the solute were then calculated assuming linear concentration dependencies. The nonlinearities and light intensities were calibrated using measurements of a 1 mm thick silica plate, for which the nonlinear refractive index $n_2 = 3 \times 10^{-16}$ cm^2 W^{-1} was assumed. Z-scan measurements were also performed at 1180 nm (8470 cm^{-1}) and 1300 nm (7690 cm^{-1}) using a 775 nm Ti-sapphire regenerative amplifier (Clark-MXR CPA-2001A) pumping a Light Conversion Topas optical parametric amplifier. This system provided tunable, approximately 150 fs pulses with a repetition rate that was set at 1 kHz (or 250 Hz in some measurements). For both femtosecond systems, the energy per pulse used in the experiments was limited (using a half-wave plate/polarizer combination and/or neutral density filters) to approximately 1 μJ, resulting in nonlinear phase shifts not exceeding about 1 rad for the system containing two optical cell walls and the 1 mm path solution. The w_0 parameter of the beam (the radius at the $1/e^2$ intensity point) was typically chosen to be in the range 35−50 μm. The Rayleigh length $Z_R = \pi w_0^2/\lambda$, where w_0 is the Gaussian beam waist and λ is the wavelength, was thus taken to be $Z_R > 3$ mm (which corresponds to $w_0 > 30$ μm for $\lambda = 0.8$ μm), and a "thin sample" assumption was therefore considered to be justified. In effect, one can then treat the total effect of the third-order nonlinearity of all the components of the system, the solution (solvent and dissolved materials) and the glass walls of the cell, as being an additive quantity.[96]

Picosecond Pump−Probe Studies at 527 nm. Measurements were performed with 55 ps, 527 nm (19 000 cm^{-1}) laser pulses obtained from a laser system using a Nd:YLF Coherent Antares mode-locked oscillator and a Nd:YLF regenerative amplifier providing 20 Hz repetition rate pulses at 1054 nm (9500 cm^{-1}). After frequency doubling, the 527 nm pulses of energies up to 30 μJ/pulse were split and attenuated to provide a pump beam and a much weaker probe beam that could be mechanically delayed with respect to the pump. The samples were in the form of chloroform solutions placed in a 1 mm glass cell. The pump beam spot size on the sample was about 100 μm in diameter, and so intensities on the order of gigawatts per square centimeter were used.

(83) McDonagh, A. M.; Humphrey, M. G.; Samoc, M.; Luther-Davies, B.; Houbrechts, S.; Wada, T.; Sasabe, H.; Persoons, A. *J. Am. Chem. Soc.* **1999**, *121*, 1405.
(84) Cifuentes, M. P.; Powell, C. E.; Humphrey, M. G.; Heath, G. A.; Samoc, M.; Luther-Davies, B. *J. Phys. Chem. A* **2001**, *105*, 9625.
(85) Powell, C. E.; Humphrey, M. G.; Cifuentes, M. P.; Morrall, J. P.; Samoc, M.; Luther-Davies, B. *J. Phys. Chem. A* **2003**, *107*, 11264.
(86) Powell, C. E.; Cifuentes, M. P.; Morrall, J. P. L.; Stranger, R.; Humphrey, M. G.; Samoc, M.; Luther-Davies, B.; Heath, G. A. *J. Am. Chem. Soc.* **2003**, *125*, 602.
(87) Duff, C. M.; Heath, G. A. *Inorg. Chem.* **1991**, *30*, 2528.
(88) Clays, K.; Persoons, A. *Phys. Rev. Lett.* **1991**, *66*, 2980.
(89) Clays, K.; Persoons, A. *Rev. Sci. Instrum.* **1992**, *63*, 3285.
(90) Clays, K.; Persoons, A.; De Maeyer, L. *Adv. Chem. Phys.* **1993**, *85*, 455.
(91) Heesink, G. J. T.; Ruiter, A. G. T.; van Hulst, N. F.; Bolger, B. *Phys. Rev. Lett.* **1993**, *71*, 999.
(92) Verbiest, T.; Clays, K.; Persoons, A.; Meyers, A.; Bredas, J. L. *Opt. Lett.* **1993**, *18*, 525.
(93) Verbiest, T.; Clays, K.; Samyn, C.; Wolff, J.; Reinhoudt, D.; Persoons, A. *J. Am. Chem. Soc.* **1994**, *116*, 9320.
(94) Morrison, I. D.; Denning, R. G.; Laidlaw, W. M.; Stammers, M. A. *Rev. Sci. Instrum.* **1996**, *67*, 1445.
(95) Sheik-Bahae, M.; Said, A. A.; Wei, T.; Hagan, D. J.; van Stryland, E. W. *IEEE J. Quantum Electron.* **1990**, *26*, 760.
(96) Samoc, M.; Samoc, A.; Luther-Davies, B.; Humphrey, M. G.; Wong, M.-S. *Opt. Mater.* **2002**, *21*, 485.

Electroabsorption Studies. The complexes were dissolved in a chloroform solution of poly(methyl methacrylate) (PMMA) and spin-coated onto an indium−tin oxide (ITO)-coated glass substrate. The thicknesses of the films were in the range 1.8−3.0 μm, and the concentrations of the complexes were ca. 4 wt %, except for **7c** and **7d**, for which the concentrations were 1.0 and 2.0 wt %, respectively, due to their low solubility. The number densities of the complexes in the films were (7.8−8.7) × 10^{18} cm^{-1} for **5a**−**d**, 2.8 × 10^{18} cm^{-1} for **6a** and **6b**, 2.5 × 10^{19} cm^{-1} for **7a** and **7b**, 5.5 × 10^{18} cm^{-1} for **7c**, and 1.1 × 10^{19} cm^{-1} for **7d**. To form a sandwich structure, semitransparent gold electrodes were evaporated onto the film in each case. White light from a tungsten−halogen lamp was monochromated and incident to the film, and the transmitted light was detected by a photodiode. A low-frequency (137.5 Hz) electric field of ca. 2 × 10^5 V cm^{-1} was applied normal to the film, and modulation in the transmitted light intensity at the doubled frequency (275 Hz) was detected by a lock-in amplifier, so that the third-order NLO response, which is proportional to the square of the applied electric field, was probed. Measurements were performed in the regions 350−550 or 350−800 nm, depending on the specific complex.

Electrochemical Switching of Cubic Nonlinearity. Argon-saturated dichloromethane solutions containing ca. 0.3 M $(NBu^n_4)PF_6$ supporting electrolyte were examined in an OTTLE cell (with Pt auxiliary, Pt working, and Ag−AgCl reference electrodes), path length 0.5 mm, with the 800 nm (12 500 cm^{-1}) laser beam passing through a focusing lens and directed along the axis passing through a 1.5 mm diameter hole in the Pt sheet working electrode. The electrochemical cell was mounted on a computer-driven translation stage, as usual in Z-scan measurements.[95] The beam waist w_0 was chosen similar to our standard Z-scan measurements (30−45 μm). The beam "cropping" by the aperture was therefore negligible over the range of travel of the cell ($z = -3$ to $+3$ cm from the focal plane), the beam radius growing by roughly a factor of 10 (i.e., to about 300−450 μm) over the distance of 10 Rayleigh lengths, but still providing for almost complete transmission. The beam transmitted through the electrochemical cell was split in two, one part being focused on an "open aperture" detector, the other part being transmitted through a 1 mm aperture to provide the "closed aperture" signal. Z-scans were collected with the appropriate potential applied to this electrochemical cell. The electrogeneration potential was 0.8 V to ensure complete electrolysis; this required approximately 5 min. Z-scan measurements were carried out during the electrolysis and were continued while the electrode potential was cycled from 0 to 0.8 V and back to zero again. The real and imaginary parts of the nonlinear phase change were determined by numerical fitting using equations given in the literature,[95] assuming that the absorption saturation process can be modeled by a linear dependence of the absorption coefficient on the light intensity.[97] The nonlinearities and light intensities were calibrated using measurements of a 1 mm thick silica plate as above. A similar setup was employed at other wavelengths (1.18 and 1.3 μm were used).

Femtosecond DFWM and Pump−Probe Studies at 800 nm. The amplified Ti-sapphire laser system was used to supply 800 nm femtosecond pulses at 30 Hz. The beam from the laser was split into three beams. Two beams (beams 1 and 2) were timed to arrive at the sample (a hole in the Pt electrode) simultaneously, while the delay of a third beam (beam 3) was scanned with a computer-controlled delay line. The folded BOXCARS geometry was used.[97] The phase-matched DFWM signal, appearing in the fourth corner of the rectangle defined by the three incident beams, was monitored as a function of the beam 3 delay. The intensity of beam 3 transmitted through the sample was also monitored: this provided a pump−probe (transient absorption, TA) signal, where beams 1 and 2 were pumps and beam 3 was the probe monitoring transmission changes induced by the pump beams.

(97) Sutherland, R. L. *Handbook of Nonlinear Optics*; Marcel Dekker: New York, 1996; Vol. 52.

Results and Discussion

Linear Optical, Electrochemical, and Spectroelectrochemical Behavior. The complexes and compounds chosen for the present study are shown in Figure 1. The systematic variation inherent in these compounds permits assessment of the effects of sequential replacement of chloro by alkynyl ligand, chain lengthening of alkynyl ligand, introduction of ligated metal center, π-system lengthening through the metal center, peripheral group modification, and progression from linear to octupolar and dendritic compounds on the electrochemical, linear, and nonlinear optical properties. Cyclic voltammetry studies revealed that the complexes undergo reversible oxidation in solution (Table 1), assigned to the $Ru^{II/III}$ couple [$i_{pc}/i_{pa} \approx 1$, $\Delta E_p(Ru^{II/III}) \approx \Delta E_p$(ferrocene/ferrocenium)]. As expected, introduction of a peripheral acceptor group (proceeding from **7b** to **7c**, **5b** to **5c**, and **6a** to **6b**) results in an increase in $E_{1/2}$, and introduction of a peripheral donor group (proceeding from **7b** to **7d**, and **5b** to **5d**) results in a decrease in the $Ru^{II/III}$ oxidation potential; electron density at the metal center is therefore tunable. Replacing chloro by phenylalkynyl ligand (proceeding from **7a** to **7b**, and **5a** to **5b**) results in little change in $E_{1/2}$, consistent with the phenylalkynyl ligand behaving as a pseudo-halide. Progression from linear fragment to octupolar complex (**7a** to **5a**, **7b** to **5b**, **7c** to **5c**, and **7d** to **5d**), and replacing octupolar compound by dendritic complex (proceeding from **5b** to **6a**, and **5c** to **6b**), also result in little change in the ease of oxidation. The octupolar and dendritic compounds **5a**−**d** and **6a**,**b** evince one oxidation process only, consistent with the extended π-system and meta substitution at the central ring resulting in non-communicating metal centers.

The UV−vis−NIR absorption data are listed in Table 1. All non-nitro-containing complexes are optically transparent at frequencies <20 000 cm^{-1}, whereas spectra of the nitro-containing compounds contain a low-energy band with ν_{max} at ca. 20 300 cm^{-1} and ν_{onset} at ca. 17 500 cm^{-1}. We have employed density functional theory (DFT) calculations on models of the linear compounds to assign the low-energy bands of the phenylalkynyl complexes as MLCT, and specifically Ru $d_{yz} \rightarrow C_2R$, in nature;[86] introduction of a nitro substituent will lower the energy of the alkynyl-centered orbital, consistent with the optical spectra. Progression from the linear complexes **7a**−**d** to the octupolar complexes **5a**−**d** results in little change in optical absorption maxima. A small gain in transparency is seen on proceeding from octupolar **5b** to dendritic **6a**, which may indicate that the dendritic complex **6a** has a non-planar geometry. This onset of non-coplanarity is consistent with an increase in the size of a dendritic system resulting in a progression from planar to globular disposition.

The Ru^{III} complexes can be conveniently generated electrochemically in dichloromethane using an OTTLE cell. A representative progression (for conversion of **5a** to $\mathbf{5a}^{3+}$) is depicted in Figure 2, while relevant spectroscopic data for all complexes and their oxidized forms are collected in Table 1. All Ru^{II} complexes are essentially transparent at frequencies below 17 000 cm^{-1}, while the Ru^{III} complex cations have a strong absorption band in the NIR; we have assigned this band by DFT calculations on model complexes of **7a** and **7b** to alkynyl-to-Ru^{III} charge transfer.[86] As expected, the ligand set about the ruthenium influences the optical absorption maximum in the Ru^{III} complexes; the chloro-alkynyl complexes $\mathbf{5a}^{3+}$ and

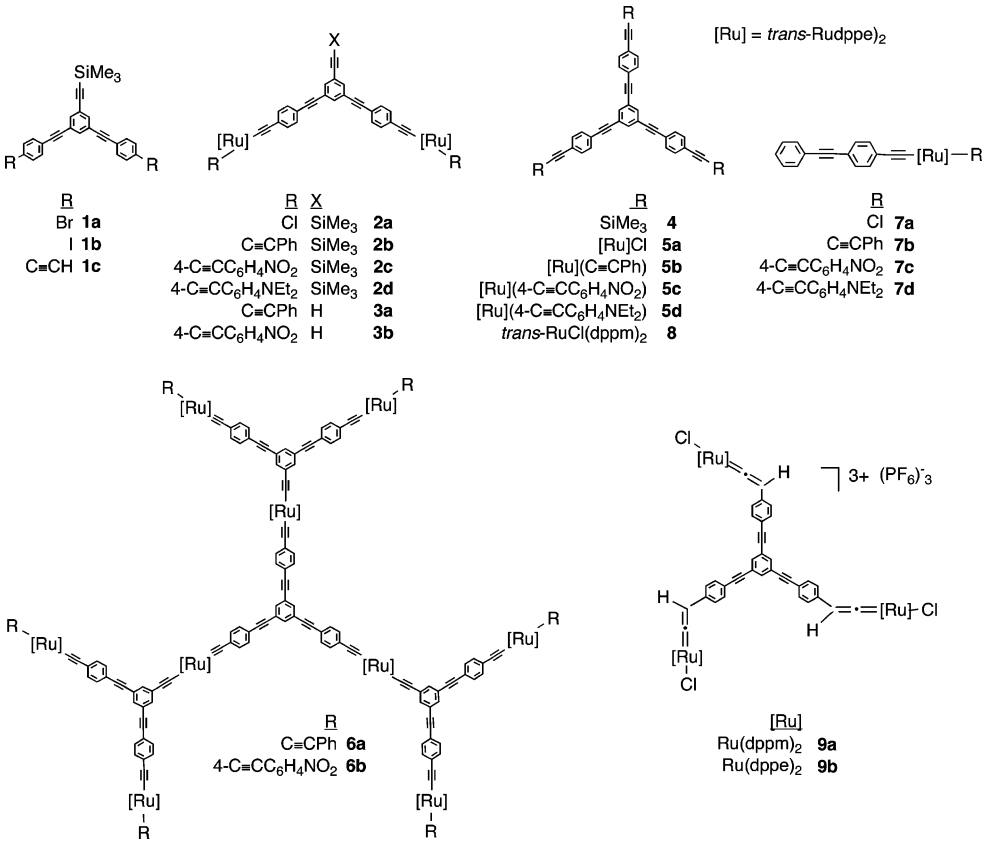

Figure 1. Alkynylruthenium complexes examined in this work.

Table 1. Cyclic Voltammetric and Linear Optical Data in CH_2Cl_2 for Complexes **5a**−**d**, **6a**,**b**, and **7a**−**d**

	$E_{1/2}$ [i_{pc}/i_{pa}, ΔE_p],[a] $Ru^{II/III}$	ν_{max} [ϵ],[b] Ru^{II}	ν_{max} [ϵ],[b] Ru^{III}	ref
7a	0.55 [1, 0.06]	25 760 [3.6]	11 160 [2.0]	86
7b	0.56 [1, 0.07]	25 540 [6.8]	8 440 [2.9]	86
7c	0.66 [1, 0.07]	20 300 [2.6]	8 720 [2.8]	this work
7d	0.23 [1, 0.06]	25 100 [4.3]	8 840 [3.3]	this work
5a	0.51 [1, 0.06]	24 200 [12.2]	11 200 [7.8]	this work
5b	0.54 [1, 0.06]	24 000 [13.1]	8 430 [7.6]	this work
5c	0.66 [1, 0.06]	21 800 [8.9]	n.d.	this work
5d	0.23 [1, 0.06]	24 340 [10.1]	8 800 [6.9][c]	this work
6a	0.58 [1, 0.07]	24 200 [39.6]	8 340 [30.1]	this work
6b	0.67 [1, 0.08]	21 400 [16.0]	n.d.	this work

[a] Ag/AgCl reference electrodes (ferrocene/ferrocenium couple located at 0.56 V, $\Delta E_p = 0.06$ V); $E_{1/2}$, ΔE_p in V. [b] ν_{max} in cm^{-1}, [ϵ] in 10^4 M^{-1} cm^{-1}. [c] Oxidation carried out using 4.5 equiv of ferrocenium at room temperature; sample was decomposing. n.d. = not determined.

7a$^+$ evince maxima at ca. 11 200 cm^{-1}, whereas spectra of the dialkynyl complex cations possess maxima at ca. 8500 cm^{-1}.

Quadratic Hyperpolarizabilities. We have determined the molecular quadratic nonlinearities, β, of the non-diethylamino-functionalized complexes and relevant organic compounds using the HRS technique at 1064 nm, the data from which are presented in Table 2. The first hyperpolarizability data are reported as the square-roots of the rotational averages. In the HRS experiment, measurements of the rotational averages are made, where $\langle\beta^2\rangle$ results from averaging over all possible orientations in an isotropic solution. Hence, in general, $\langle\beta^2\rangle$ is a function of all non-zero hyperpolarizability tensor components. For one-dimensional purely dipolar molecules, only the diagonal tensor component along the molecular 3-axis, β_{333}, is significant, so that $\beta = \sqrt{(6/35)}\beta_{333}$. For octupolar molecules with D_{3h}, T_d, or D_{2d} symmetry, the only non-zero hyperpolarizability tensor component is β_{123}. For the D_{3h}-symmetric complexes in the present study, $\beta = \sqrt{(8/21)}\beta_{123}$. No β values could be collected for **7c** because of insufficient solubility. Complex **5a** was measured at both Leuven and RIKEN, with consistent results at the two laboratories.

The complexes bearing no nitro substituents have absorption bands relatively far from the second-harmonic wavelength of 532 nm, permitting assessment of the impact of structural variation on quadratic NLO merit. Incorporation of the ligated metal fragment in proceeding from the organic acetylenes **4** and **1c** to the organometallic complexes **5a** and **2a** leads to a significant increase in β_{HRS}. Extending the delocalized π-system through the metal in progressing from **5a** to **5b** and **2a** to **2b**, though, is ineffective in increasing β, indicating that the *trans*-phenylalkynyl ligand is acting largely as a π-donor ligand (we have previously reported that phenylalkynyl ligands are pseudo-halides in complexes of this type);[98] a similar lack of β enhancement on extending the π-system through a metal has been reported in a dipolar system.[99] Replacing diphosphine co-ligand dppe by dppm in proceeding from **5a** to **8** or **9b** to **9a** results in a significant decrease in β value, consistent with a decrease in extinction coefficient of the low-energy optical absorption band. Converting these alkynyl complexes to the corresponding vinylidene complexes in proceeding from **5a** to **9b** or **8** to **9a** results in a slight decrease in β value, but not of sufficient magnitude for these complexes to be of interest as

(98) McGrady, J. E.; Lovell, T.; Stranger, R.; Humphrey, M. G. *Organometallics* **1997**, *16*, 4004.
(99) Coe, B. J.; Harris, J. A.; Harrington, L. J.; Jeffery, J. C.; Rees, L. H.; Houbrechts, S.; Persoons, A. *Inorg. Chem.* **1989**, *28*, 3391.

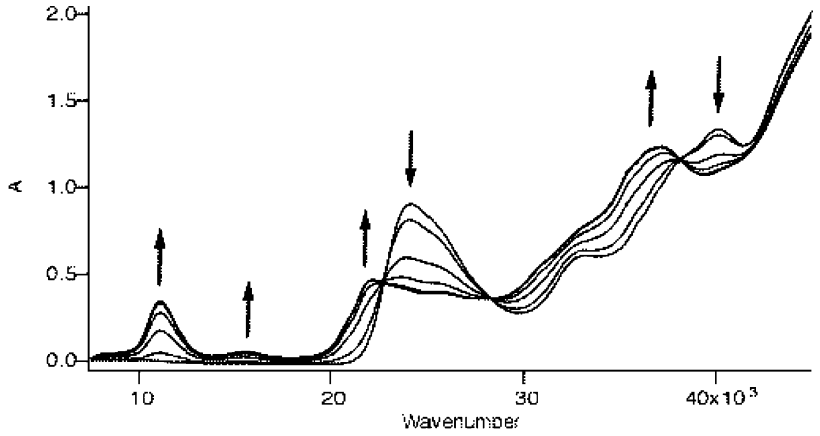

Figure 2. UV−vis−NIR spectra of a CH_2Cl_2 solution of **5a** in an OTTLE cell, path length 0.5 mm, during oxidation at $E_{appl} \approx 0.80$ V at 248 K.

Table 2. Linear and Quadratic Nonlinear Optical Data at 1064 nm in Tetrahydrofuran

	λ_{max}, ϵ[a]	$\sqrt{\langle\beta^2\rangle}$[b]	$\sqrt{\langle\beta_0^2\rangle}$[b]		λ_{max}, ϵ[a]	$\sqrt{\langle\beta^2\rangle}$[b]	$\sqrt{\langle\beta_0^2\rangle}$[b]
1a	311, 7.6	6	4	**5a**	413, 9.9	94[c]/115	32/39
1b	314, 8.1	9	5	**5b**	412,11.6	93[c]	31
1c	322, 8.6	8	5	**5c**	459, 8.9	1220	254
2a	412, 7.3	101	34	**6a**	402, 42.1	160	59
2b	408, 7.5	105	37	**6b**	467, 16.0	1880	350
2c	461, 5.9	900	182	**7b**	382, 3.8	34[c]	14
3a	407, 8.1	104	37	**8**	404, 5.6	31	11
3b	463, 6.2	1120	220	**9a**	415, 0.9	19	6
4	342, 0.5	8[c]	4	**9b**	414, 2.4	84	28

[a] λ_{max} in nm, ϵ in 10^4 M^{-1} cm^{-1}. [b] In 10^{-30} esu, measured at 1064 nm, values ±10%. [c] Measured at RIKEN, Japan.[83]

protically switchable NLO materials.[100] Complex **7b** is a linear fragment of the octupolar complex **5b**, and also of the wedge complexes **2b** and **3a**. Not surprisingly, progressing from **7b** to **5b** results in a 3-fold increase in oscillator strength of the UV−vis band assigned to the MLCT transition, while progressing from **7b** to **2b** or **3a** results in a 2-fold increase in the same parameter. Importantly, the quadratic NLO merit of two-dimensional complex **5b** is significantly improved compared to the one-dimensional complex **7b**, with little loss of optical transparency (in progressing from **7b** to **5b**) accompanying the large increase in β. A similar increase in β is also seen in complexes **2b** and **3a**, although these complexes contain only two metal centers, compared with three for **5b**.

The dendrimer **6a** results from the coupling of **5a** and **3a**. While its β value is larger than that of either of the component complexes, it is not substantially so, bearing in mind that it contains nine metal centers, compared to three or two for the components. Improvements in nonlinearity in dipolar systems are usually accompanied by a loss in optical transparency. The present "multipolar" system is significant, in that there is no loss in transparency on progressing from **5b** to **6a**. The absolute values of β_{HRS} for **5b** and **6a** are very large for multipolar compounds that are optically transparent at the second-harmonic, for which resonance enhancement is much less important. They are also very large for multipolar compounds lacking a formal acceptor moiety at the core (results with organic compounds suggest that a further increase in β is likely upon replacing the central arene ring with an electron acceptor such as 2,4,6-trinitroaryl or 2,4,6-triazine groups).[101,102]

The measured β values of the nitro-containing complexes are an order of magnitude greater that those of their non-nitro analogues. The β values of the nitro-containing complexes are, however, strongly resonance enhanced due to the proximity of the absorption band associated with the MLCT transition (assigned to the metal-to-nitrophenylalkynyl ligand charge transfer) to the second-harmonic wavelength of 532 nm (18 800 cm^{-1}). Complexes **2c** and **3b** each contain two metal centers, and they possess similar β values. Only a small increase in β is observed on progressing to the three-metal-center complex **5c**, similar to the trend observed for the non-nitro analogues. A 50% gain in β is found on progressing from **5c** to the nine-metal-center dendrimer **6b**. The β value of 1880 × 10^{-30} esu for the latter is large for an octupolar molecule (cf., for example, the inorganic octupolar complex reported by Dhenaut et al.),[103] but as mentioned above, this is due in part to resonance enhancement.

The method used to calculate static β values for dipolar complexes is based on the two-level description of β.[104] It has long been recognized that the simple two-level model[105−107] is inadequate when an absorption band approaches either the second-harmonic or fundamental incident radiation wavelengths, because one does not adequately account for damping effects.[105] One approach to refine the two-level model considers the impact of vibrational sub-states of the electronic ground and excited states.[108−110] Other attempts to more correctly describe the dispersion of the first hyperpolarizability take the damping and the resulting imaginary part of the hyperpolarizability into account.[108−113] None of these approaches has been shown to accurately predict the experimental dispersion effects of a simple charge-transfer chromophore having a single CT absorption

(100) Hurst, S.; Cifuentes, M. P.; Morrall, J. P. L.; Lucas, N. T.; Whittall, I. R.; Humphrey, M. G.; Asselberghs, I.; Persoons, A.; Samoc, M.; Luther-Davies, B.; Willis, A. C. *Organometallics* **2001**, *20*, 4664.
(101) Wortmann, R.; Glania, C.; Krämer, P.; Matschiner, R.; Wolff, J. J.; Kraft, S.; Treptow, B.; Barbu, E.; Längle, D.; Görlitz, G. *Chem. Eur. J.* **1997**, *3*, 1765.
(102) Hennrich, H.; Asselberghs, I.; Clays, K.; Persoons, A. *J. Org. Chem.* **2004**, *69*, 5077.
(103) Dhenaut, C.; Ledoux, I.; Samuel, I. D. W.; Zyss, J.; Bourgault, M.; Bozec, H. L. *Nature* **1995**, *374*, 339.
(104) Di Bella, S. *New J. Chem.* **2002**, *26*, 495.
(105) Oudar, J. L.; Chemla, D. S. *J. Chem. Phys.* **1977**, *66*, 2664.
(106) Oudar, J. L. *J. Chem. Phys.* **1977**, *67*, 446.
(107) Willetts, A.; Rice, J. E.; Burland, D. M.; Shelton, D. P. *J. Chem. Phys.* **1992**, *97*, 7590.
(108) Pauley, M. A.; Wang, C. H. *Rev. Sci. Instrum.* **1999**, *70*, 1277.
(109) Wang, C. H. *J. Chem. Phys.* **2000**, *112*, 1917.
(110) Woodford, J. N.; Wang, C. H.; Jen, A. K. Y. *Chem. Phys.* **2001**, *271*, 137.
(111) Berkovic, G.; Meshulam, G.; Kotler, Z. *J. Chem. Phys.* **2000**, *112*, 3997.
(112) Meshulam, G.; Berkovic, G.; Kotler, Z. *Rev. Sci. Instrum.* **2000**, *71*, 3490.
(113) Meshulam, G.; Berkovic, G.; Kotler, Z. *Opt. Lett.* **2001**, *26*, 30.

band. The situation for octupolar molecules is even more complex. The term $\Delta\mu$, which is the difference between the ground- and excited-state dipole moments, must be zero for octupolar molecules. A three-level model has been proposed that incorporates a doubly degenerate excited state with a dipole-allowed transition between the ground and the excited states.[114] Due to the degeneracy of the excited states, an expression for β_0 is obtained that resembles the two-level expression, so that (excluding constants)[115,116]

$$\beta \propto \frac{\omega_{eg} f \mu_{1\bar{1}}}{(\omega_{eg}{}^2 - \omega^2)(\omega_{eg}{}^2 - (2\omega)^2)}$$

where ω_{eg} is the frequency of the optical transition, f is the oscillator strength, ω is the frequency of the exciting radiation, and $\mu_{1\bar{1}}$ is the transition dipole moment between the two degenerate excited states. The resonant term is the simple expression from the two-level model, so that the equation

$$\beta_0 = \beta\left(1 - \left(\frac{\lambda_{max}}{\lambda}\right)^2\right)\left(1 - \left(\frac{2\lambda_{max}}{\lambda}\right)^2\right)$$

may be used to calculate static first hyperpolarizabilities, β_0. These have been calculated for the complexes listed above and are collected in Table 2. For the complexes containing nitro groups, no changes in the trends found in the experimental data are seen in the calculated static β values. The β_0 value for **6b** is among the largest obtained for an organometallic complex to date, or indeed for any molecule with formally octupolar symmetry.[117] For the complexes without nitro substituents, the static β values for the two-metal-center complexes **2a** and **3a** are marginally larger than that of the three-metal complex **5b**. No other changes in the trends discussed above are observed.

The tensorial nature of β may be used to obtain information about the symmetry of the molecule being measured. Depolarization measurements involve measuring the intensity of the scattered second-harmonic light parallel, $I_{zz}^{2\omega}$, and perpendicular, $I_{zx}^{2\omega}$, to the plane of the incident polarized laser beam. The ratio of these two quantities is dependent on the molecular symmetry.[91−94,118] For purely dipolar molecules with C_{2v} symmetry,

$$\rho = I_{zz}^{2\omega}/I_{zx}^{2\omega} = 5$$

and for purely octupolar molecules with symmetry D_{3h}, T_d, or D_{2d},

$$\rho = I_{zz}^{2\omega}/I_{zx}^{2\omega} = 1.5$$

Depolarization measurements were undertaken for complexes **5a** and **5b**. The depolarization ratio of 1.4 ± 0.2 for complex **5a** is within experimental error of the value expected for purely octupolar symmetry. Complex **5b** has a depolarization ratio of 2.1 ± 0.1, a value larger than that expected for a molecule with octupolar symmetry. This increased value may result from a deviation from octupolar symmetry, most likely a lack of coplanarity of the peripheral phenylethynyl groups with the central π-system. A decrease in molecular symmetry would result in an increase in ρ because dipolar contributions to the first hyperpolarizability are introduced. A similar observation was noted with 2,4,6-tris{4-(*N*,*N*-diethylamino)phenyl}-1,3,5-triazine and attributed to symmetry-lowering molecular distortions or conformational distributions.[101]

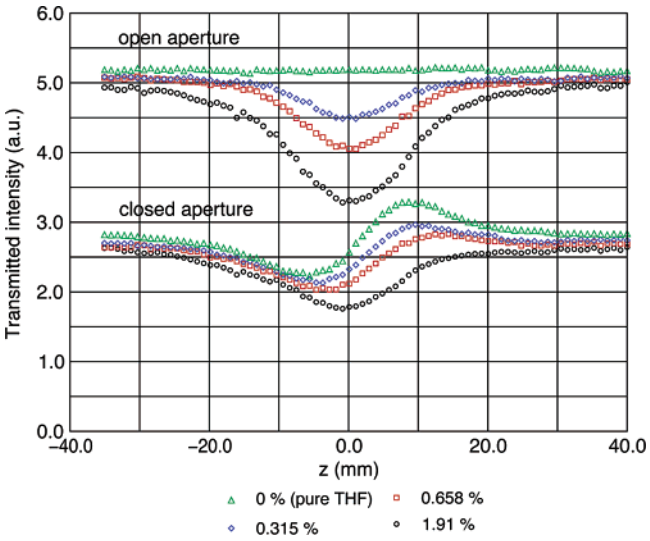

Figure 3. Z-scan measurements on solutions of **5c**, with concentrations as % w/w. The $1/e^2$ Gaussian beam spot size radius at the focus, w_0, is about 49 μm.

Cubic Hyperpolarizabilities. We have determined third-order optical nonlinearities using the Z-scan technique at 800 nm (12 500 cm^{-1}); the linear complex **7c** was not measured because it was insufficiently soluble in the range of suitable solvents. Figure 3 shows experimental data plots from the Z-scan experiment on solutions of **5c**. The Gaussian beam spot size radius at the focus, w_0, is about 49 μm. The upper set of curves in Figure 3 shows the open-aperture experiment for various concentrations. They reveal a significant increase in absorption with increasing beam intensity (i.e., there is a reduction in transmittance as the sample approaches $z = 0$). This is indicative of two-photon absorption (TPA). From these curves, the nonlinear absorption coefficient β_2 and the related imaginary part of γ may be calculated, and the results are given in Table 3. Values of the TPA cross section, σ_2, may also be calculated from β_2, and these are included in Table 3. [Note that the Z-scan measurements were performed using low repetition rate (30 Hz), 100 fs pulses; excited-state absorption should therefore be negligible.] The bottom set of curves in Figure 3 show results from the closed-aperture experiment (performed concurrently with the open-aperture experiment). The shapes of the curves (i.e., the presence of a valley at $z < 0$, followed by a maximum at $z > 0$) indicate a positive (self-focusing) refractive nonlinearity of the solution, with the growing asymmetry of the curves being due to the increasing significance of two-photon absorption. However, analysis of the concentration dependence of these curves reveals that the refractive nonlinearity of the solution decreases with the concentration of the solute, and thus a self-defocusing nature of the complex is found at this wavelength. From these data, the real component of γ is obtained.

The significant γ_{imag} values in Table 3 are indicative of efficient TPA. The effect becomes important as 2ω (i.e., twice

(114) Joffre, M.; Yaron, D.; Silbey, R. J.; Zyss, J. *J. Chem. Phys.* **1992**, *97*, 5607.
(115) Zyss, J.; Dhenaut, C.; Chauvan, T.; Ledoux, I. *Chem. Phys. Lett.* **1993**, *206*, 409.
(116) Wolff, J.; Wortmann, R. *Adv. Phys. Org. Chem.* **1999**, *32*, 121.
(117) Lee, M.-J.; Piao, M.; Jeong, M.-Y.; Lee, S. H.; Kang, K. M.; Jeon, S.-J.; Lim, T. G.; Cho, B. R. *J. Mater. Chem.* **2003**, *13*, 1030.
(118) Vance, F. W.; Hupp, J. T. *J. Am. Chem. Soc.* **1999**, *121*, 4047.

Table 3. Linear and Cubic Nonlinear Optical Data

complex	λ_{max}, ϵ[a]	γ_{real}[b]	γ_{imag}[b]	$\lvert\gamma\rvert$[b]	σ_2[c]
1a	311, 7.6	53 ± 20	5 ± 3	53 ± 20	1 ± 1
1b	314, 8.1	77 ± 30	4 ± 3	77 ± 30	1 ± 1
1c	322, 8.6	67 ± 30	7 ± 5	67 ± 30	2 ± 1
2a	412, 7.3	−510 ± 500	4700 ± 1500	4700 ± 1500	1100 ± 360
2b	408, 7.5	−700 ± 100	2270 ± 300	2400 ± 300	550 ± 70
2c	461, 5.9	−5200 ± 1000	5200 ± 1000	7400 ± 1400	1300 ± 250
2d	410, 7.7	−3300 ± 1300	4600 ± 900	5700 ± 1500	1000 ± 200
3a	407, 8.1	−830 ± 100	2200 ± 300	2400 ± 300	530 ± 70
3b	463, 6.2	−4900 ± 1000	4900 ± 1000	6900 ± 1400	1200 ± 250
4	342, 0.5	95 ± 20	0	95 ± 20	0
5a	413, 9.9	−330 ± 100	2200 ± 500	2200 ± 500	530 ± 100
5b	412,11.6	−600 ± 200	2900 ± 500	3000 ± 500	700 ± 120
5c	459, 8.9	−5000 ± 1000	5600 ± 1000	7500 ± 1400	1300 ± 200
5d	410, 15.3	−8300 ± 3000	5300 ± 1000	9500 ± 3100	1300 ± 200
6a	402, 42.1	−5050 ± 500	20100 ± 2000	20700 ± 2100	4800 ± 500
6b	467, 16.0	−14900 ± 3000	18200 ± 3000	23500 ± 4200	4400 ± 700
7a	388, 3.6	−100 ± 100	450 ± 200	460 ± 200	110 ± 50
7b	382, 3.8	−670 ± 300	1300 ± 300	1500 ± 400	310 ± 70
7d	386, 2.3	−1300 ± 1000	−3200 ± 500	3500 ± 800	−760 ± 120

[a] λ_{max} in nm, ϵ in 10^4 M^{-1} cm^{-1}. [b] In 10^{-36} esu. [c] Goeppert-Mayers = 10^{-50} cm^4 s. Calculated using $\sigma_2 = \hbar\omega\beta_2/N$, where $\hbar$ is Planck's constant divided by 2π, ω is the exciting frequency, β_2 is the two-photon absorption coefficient, and N is the concentration.

the exciting laser frequency, in this case 25 000 cm^{-1} or 400 nm) approaches the positions of two-photon-allowed transitions to excited states. Without performing a full study of the dispersion of γ_{imag},[1] it is difficult to know if these coincide with one-photon (linear absorption) transitions. However, the close proximity to 2ω of the absorption band assigned to a MLCT transition for **6a** may be important for the particularly large values of γ_{imag} and σ_2 for this complex. The negative γ_{real} values in Table 3 are likely to result from two-photon dispersion effects (resonant behavior of the cubic hyperpolarizability involves a rapidly changing real part and an enhanced imaginary part), but one cannot completely exclude the possibility that negative zero-frequency contributions to the cubic hyperpolarizabilities are of some importance. [Note, though, that the organic compound **4**, which exhibits no TPA at 800 nm, has a positive γ_{real} value.] While it is likely that the negative γ_{real} values result from two-photon dispersion effects, the sign of γ_{real} is quite sensitive to small differences in the energies of absorption bands of the complexes. This is a reason why comparisons of values of nonlinearities of two-photon-absorbing molecules are quite difficult. Some insight can be gained when looking at changes in the modulus of the hyperpolarizability, $|\gamma|$, which is less sensitive to dispersion than the components γ_{real} and γ_{imag}. With these reservations, we note that, not unexpectedly, introduction of the ligated metal on proceeding from **4** to **5a** or **1c** to **2a** results in significant increases in γ_{real}, γ_{imag}, and $|\gamma|$. Inspection of γ values for **7b** and **5b** reveals a significant increase in the imaginary component on progressing from the linear to the multipolar complex, but no increase in γ_{real}. Both real and imaginary components of the third-order hyperpolarizability for the dendrimer **6a** are much larger than those of its components **3a** and **5a** or the related complex **5b**. In particular, progressing from **5b** to **6a** results in increases in both γ_{real} and γ_{imag} proportionately greater than increase in either the the number of phenylethynyl groups or the extinction coefficient. Comparison of the nitro-containing complexes **5c**, **2c**, and **3b** to their non-nitro analogues reveals large increases in both real and imaginary γ values. Comparison of the dendrimer complexes shows a large increase in γ_{real}, but no change in γ_{imag}, on progressing from **6a** to **6b**. These results suggest that the introduction of a nitro group has a significant effect on the cubic nonlinearity, but the degree to which this is affected by two-photon dispersion is not readily ascertained from these data.

Table 4. One- and Two-Photon Absorption Cross Sections for Selected Complexes

	7b	**2b**	**3a**	**5b**	**6a**
σ[a]	6	13	14	19	70
σ/MW[b]	5.0	5.4	6.0	5.5	6.9
σ_2[c]	310	550	530	700	4800
σ_2/MW[d]	0.26	0.23	0.23	0.20	0.47

[a] σ in 10^{-17} cm^2. [b] σ/MW in 10^{-20} cm^2 mol g^{-1}. [c] σ_2, GM = 10^{-50} cm^4 s; error ∼15%. [d] σ_2/MW, 10^{-50} cm^4 s mol g^{-1}; error ∼15%.

Table 4 contains one- and two-photon absorption cross sections, together with these parameters divided by the molecular weight (MW), for complexes **2b**, **3a**, **5b**, **6a**, and **7b**; these complexes were chosen to examine the effect of changing geometry and molecular size on linear and nonlinear absorption properties because each metal center has an almost identical ligand environment, and similar UV−vis absorption bands are observed in the region close to 2ω. The one-photon absorption cross sections (which are proportional to the molar extinction coefficients) follow the expected ordering **6a** > **5b** > **2b** ≈ **3a** > **7b**, i.e., the complexes containing nine, three, two, two, and one metal center, respectively. With the exception of **6a**, the one-photon absorption cross sections scale with the number of metal centers in each complex (∼6 × 10^{-17} cm^2 per metal center). For the dendrimer **6a**, this scaling factor does not hold, a higher figure per metal center being observed. This trend is reflected in the σ/MW values, with the complexes with one, two or three metal centers ranging from 5.0 × 10^{-20} to 6.0 × 10^{-20} cm^2 mol g^{-1}, but with **6a** having a value of 6.9 × 10^{-20} cm^2 mol g^{-1}. Examination of the TPA cross sections reveals the same ordering as for the linear absorption parameter, with complexes **2b**, **3a**, **5b**, and **7b** having σ_2 values between 200 × 10^{-50} and 300 × 10^{-50} cm^4 s per metal center, but complex **6a** having a value of ∼500 × 10^{-50} cm^4 s per metal center. Similarly, the σ_2/MW values reveal a larger TPA coefficient per unit of molecular mass for the dendrimer complex **6a** than for the smaller related complexes. Clearly, both linear and nonlinear absorption characteristics are altered upon proceeding

Table 5. Experimental Cubic NLO Response Parameters in Solid Solution in PMMA Measured by Electroabsorption

compound		λ_{max} (nm)	Im($\chi^{(3)}$)/N^a [negative peak]^b	Im($\chi^{(3)}$)/N^a [positive peak]^b	$\Delta\mu^c$
5a		414	−230 [424]	200 [457]	29
5b		410	−200 [423]	140 [463]	27
5c	(peak-1)	406	−290 [416]	210 [448]	46
	(peak-2)	468	−150 [494]	150 [562]	
5d		408	−320 [428]	230 [470]	56
6a		410	−590 [423]	370 [458]	29
6b	(peak-1)	400	−240 [408]	180 [455]	23
	(peak-2)	(480)^d	−140 [501]	160 [575]	
7a		386	−50 [400]	57 [432]	33
7b		384	−66 [400]	65 [430]	33
7c	(peak-1)	376	−47 [388]	45 [424]	31
	(peak-2)	478	−42 [488]	34 [562]	
7d		386	−74 [404]	66 [442]	38

^{a} $\chi^{(3)}$ was normalized by the number density of the molecules N (cm^{-3}) in PMMA matrix, to remove the concentration dependence. Im($\chi^{(3)}$)/N is given in 10^{-33} esu cm^3. ^{b} Wavelength for the peak value, given in nm.^{c} $\Delta\mu$, the difference between the ground- and excited-state dipole moments, is given in D and was obtained through fitting the electroabsorption spectrum by the second derivative of the absorption spectrum. ^{d} A shoulder rather than a peak.

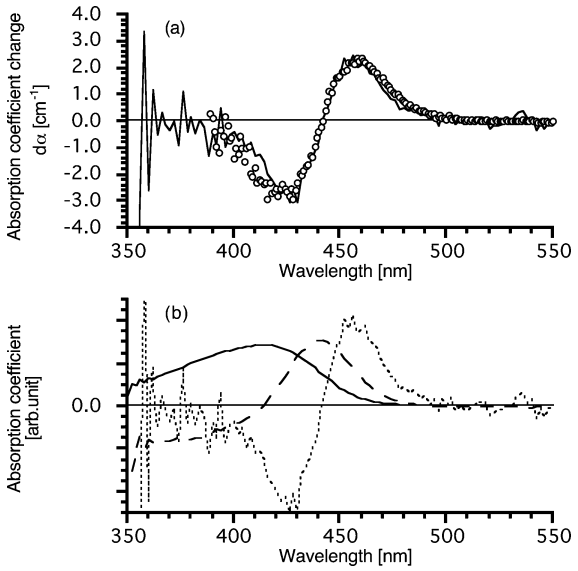

Figure 4. (a) Electroabsorption spectrum of a solid solution of **5a** (4.0% w/w in PMMA) (open circles) and the result of curve-fitting (full line). (b) First (dashed line) and second (dotted line) derivatives of the linear absorption spectrum (full line) of the same sample. The derivatives were arbitrarily scaled for comparison of the profile.

from the smaller ruthenium−alkynyl complexes to the dendrimer. Both of the dendritic complexes **6a** and **6b** show σ_2 values comparable in magnitude to the highest values reported for organic conjugated systems under conditions of low-repetition-rate femtosecond pulse excitation. [It should be noted that large discrepancies exist in the literature between the two-photon absorption cross section values determined using laser pulses of different duration and under different fluences, presumably due to processes such as excited-state absorption and saturation.] In the present case, it is likely that the size and two-dimensional nature of the π-delocalized system, combined with the strong MLCT transition, all contribute to the large observed σ_2 value.

Electroabsorption Studies. Third-order nonlinear susceptibilities $\chi^{(3)}$ were determined for **5a**−**d**, **6a**,**b**, and **7a**−**d** by EA spectral measurements. The measurement wavelength range was 350−550 nm (28 600−18 200 cm^{-1}), except for the nitro-substituted complexes, for which 350−800 nm (28 600−12 500 cm^{-1}) was employed due to their longer wavelength absorption bands. As we have already pointed out,[119,120] EA provides information complementary to that afforded by Z-scan. The values of Im($\chi^{(3)}$)/N can be 1−2 orders of magnitude larger than the molecular cubic nonlinearities γ obtained by Z-scan, possibly due to resonance enhancement and local field effects. The linear optical absorption maxima and Im($\chi^{(3)}$)/N values, the imaginary part of the nonlinear susceptibility normalized by the number density of molecules in PMMA matrix, are summarized in Table 5. The values of Im($\chi^{(3)}$)/N reach a negative peak at wavelengths ca. 10−20 nm longer than λ_{max} and a positive peak at wavelengths ca. 40−60 nm longer than λ_{max}. Peripheral substitution at complexes does not seem to cause large differences in Im($\chi^{(3)}$)/N values. In contrast, dimensional evolution (progressing from **7a**−**d** to **5a**−**d**) and generation increase (progressing from **5b** to **6a**) both result in 3-fold increases in Im($\chi^{(3)}$)/N values, consistent with the number increase of ligated ruthenium centers in these molecules. Complexes **6b** and **5c** are unusual in that the Im($\chi^{(3)}$)/N value for the former is smaller than that of the latter, the reason for which has not yet been elucidated.

Electroabsorption spectroscopy affords information about the character of transitions through analysis of the spectral profile: a photoinduced polarizability change affords a profile proportional to the first derivative of the absorption spectrum, and a photoinduced change in molecular dipole moment affords a profile proportional to the second derivative of the absorption spectrum.[121,122] A dominant second-derivative component corresponds to a polar transition (a charge-transfer exciton), and its absence corresponds to a nonpolar transition (a Frenkel exciton). Figure 4a shows the electroabsorption spectrum of **5a**, and Figure 4b shows derivatives of its linear absorption spectrum. It is apparent that the second derivative component is dominant, suggesting that the transition is highly polar. Other compounds also afford second-derivative-like spectral profiles. The differences between the ground- and excited-state dipole moments, $\Delta\mu$, which were derived from a curve-fitting analysis, are summarized in Table 5. All compounds possess a large $\Delta\mu$, in the range 23−56 D, possibly due to a MLCT character of the transitions.[86] Peripheral substitution of the octupolar complexes with highly polar groups (proceeding from **5a**,**b** to **5c**,**d**) results in an increase in $\Delta\mu$, but this trend is not seen with the linear (**7a**−**d**) and dendritic (**6a**,**b**) complexes. Dimensional evolution (from **7a**−**d** to **5a**−**d**) and generation increase (from **5b**,**c** to **6a**,**b**) also do not seem to evince a systematic trend. Overall, results from the EA studies suggest that each metal complex unit functions independently. A detailed analysis of the spectral profiles and anisotropy for the present series of complexes will be presented elsewhere.

Time-Resolved Picosecond Measurements. The high nonlinearities of the compounds investigated in this study suggest

(119) Hurst, S. K.; Humphrey, M. G.; Isoshima, T.; Wostyn, K.; Asselberghs, I.; Clays, K.; Persoons, A.; Samoc, M.; Luther-Davies, B. *Organometallics* **2002**, *21*, 2024.
(120) Hurst, S. K.; Lucas, N. T.; Humphrey, M. G.; Isoshima, T.; Wostyn, K.; Asselberghs, I.; Clays, K.; Persoons, A.; Samoc, M.; Luther-Davies, B. *Inorg. Chim. Acta* **2003**, *350*, 62.
(121) Feller, F.; Monkman, A. P. *Phys. Rev. B* **1999**, *60*, 8111.
(122) Videlot-Ackermann, C.; Isoshima, T.; Yassar, A.; Wada, T.; Sasabe, H.; Fichou, D. *Synth. Met.* **2006**, *156*, 154.

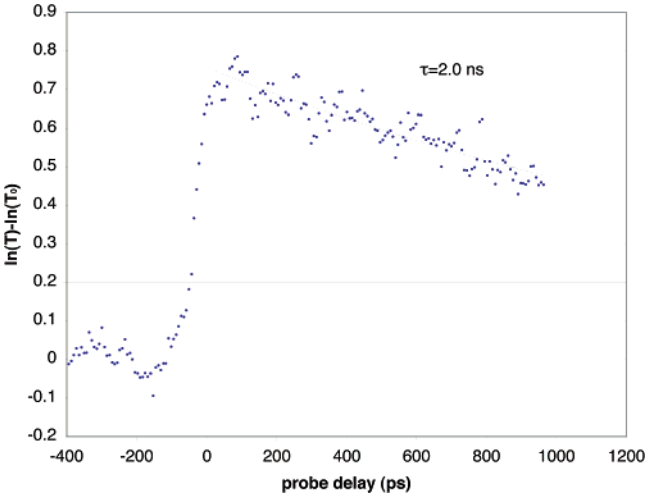

Figure 5. Induced transmission in **5c** (concentration 1.78 mg mL^{-1}, pump intensity ~3 GW cm^{-2}).

Table 6. Excited-State Lifetimes Determined from Pump−Probe Experiments at 527 nm

compound	concentration used (mg/mL)	lifetime (ns)
5c	1.78	2.0
2c	1.45	0.5
7c	2.3	0.96

optical limiting as a possible application. To probe this possibility, we have investigated nonlinear absorption in some of these compounds at a doubled neodymium laser frequency. We find, however, that the compounds **2c**, **5c**, and **7c** exhibit an absorption saturation effect when pumped at 527 nm (i.e., the pump beam transfers the population from the ground state to the excited state, with the latter having an absorption cross section lower than that of the former). The induced increase of transmission decays relatively slowly, with decay times that can be found by approximating the optical density change decay as exponential [i.e., $\Delta A(t) = \Delta A(0)\exp(-t/\tau)$]. An example of the results is given in Figure 5 and Table 6. It can be seen that the induced transmissions for these compounds have lifetimes on the order of about a nanosecond, which may be related to the lifetime of an excited state (note, however, that the dynamics of excited states may be quite complex).

Modulating Cubic Nonlinearities. Recently, the possibility of modifying molecular structure by external means and thereby switching the value of the nonlinearity has been noted. Attention has focused mainly on methods to reversibly modulate quadratic nonlinearities,[102,123] the most popular route involving photoexcitation to stimulate a structural change.[124] Molecular inorganic complexes may be particularly well-suited to certain forms of switching; their quadratic nonlinearities can potentially be switched magnetically,[125] have been irreversibly switched upon complexation,[126−129] and have been reversibly modulated by ex situ chemical oxidation and subsequent reduction,[130−132] and very recently by in situ oxidation/reduction,[133,134] but switching third-order nonlinearities of inorganic complexes is little explored.[86,100]

Oxidation of **5a** "switches on" an absorption transition that has appreciable intensity at the frequency of our mode-locked Ti-sapphire laser. To effect NLO switching, we have employed a Z-scan experiment with an incident wavelength of 800 nm (12 500 cm^{-1}), examining the materials in solution in an OTTLE cell with a switching potential of 0.8 V. The change in transmission of the open- and closed-aperture Z-scan experiment during oxidation and reduction of complex **5a** is illustrated in Figure 6. Panel (a) depicts the open- and closed-aperture traces of the neutral complex, for which strong nonlinear absorption is readily observable; it is seen to dominate the closed-aperture scan, too. Upon application of the oxidation potential (0.8 V), there is a transition period [panel (b)] where the transmission plunges (due to the growth of the strong absorption band). This decrease in transmission levels out as the complex is fully converted into the oxidized form [panel (c)]. After a sufficient time has elapsed, a new equilibrium between the oxidized and neutral complexes around the electrode is reached and the signal stabilizes [panel (d)]. At this point, the third-order properties of the oxidized complex can be determined by the usual technique of numerical fitting of the closed- and open-aperture Z-scan curves (it is assumed that the concentration of neutral molecules in the beam is very low relative to the concentration of oxidized molecules). The open-aperture scan shows a maximum at $z = 0$, indicating clearly that the solution is now acting as a saturable absorber. The potential is then changed to 0 V [panel (e)], leading to a gradual increase in the transmission (due to the loss of the strong absorption band) [panels (f) and (g)]. Panel (h) shows the endpoint, at which the neutral complex has been fully regenerated, once again showing no linear absorption but a strong two-photon absorption effect.

Table 3 reveals that octupolar complexes, such as **5a** and chemically related dendrimers, possess significant TPA cross sections σ_2 at 800 nm. The sign of the imaginary part of the third-order nonlinearity is positive in the resting state of the complex (due to the presence of TPA), but, under strong one-photon absorption conditions in the oxidized form, an absorption saturation effect is possible; it is therefore possible to reverse the sign of the absorptive nonlinearity on oxidation of **5a** and related species. By also analyzing the closed-aperture Z-scans, we find that oxidation of the molecule actually results in changes (including changes of sign) of both the imaginary (absorptive) part of the third-order nonlinearity and the real (refractive) part, which changes from negative (self-defocusing) to positive (self-focusing) nonlinearity. Importantly, cycling between the two forms of the molecule is facile. Previously reported examples of photochromic switching[135] suffer from the back-reaction proceeding thermally over hundreds of seconds, too long to be

(123) Coe, B. J. *Chem. Eur. J.* **1999**, *5*, 2464.
(124) Delaire, J. A.; Nakatani, K. *Chem. Rev.* **2000**, *100*, 1817.
(125) Gaudry, J.-B.; Capes, L.; Langot, P.; Marcen, S.; Kollmannsberger, M.; Freysz, E.; Letard, J. F.; Kahn, O. *Chem. Phys. Lett.* **2000**, *324*, 321.
(126) Di Bella, S.; Fragalà, I.; Ledoux, I.; Diaz-Garcia, M. A.; Marks, T. J. *Chem. Mater.* **1994**, *6*, 881.
(127) Di Bella, S.; Fragalà, I.; Ledoux, I.; Diaz-Garcia, M. A.; Marks, T. J. *J. Am. Chem. Soc.* **1997**, *119*, 9550.
(128) Di Bella, S.; Fragalà, I. *Synth. Met.* **2000**, *115*, 191.
(129) Fabbrini, G.; Menna, E.; Maggini, M.; Canazza, A.; Marcolongo, G.; Meneghetti, M. *J. Am. Chem. Soc.* **2004**, *126*, 6238.
(130) Coe, B. J.; Houbrechts, S.; Asselberghs, I.; Persoons, A. *Angew. Chem., Int. Ed.* **1999**, *38*, 366.
(131) Malaun, M.; Reeves, Z. R.; Paul, R. L.; Jeffery, J. C.; McCleverty, J. A.; Ward, M. D.; Asselberghs, I.; Clays, K.; Persoons, A. *Chem. Commun.* **2001**, 49.
(132) Asselberghs, I.; Clays, K.; Persoons, A.; Ward, M. D.; McCleverty, J. *J. Mater. Chem.* **2004**, *14*, 2831.
(133) Asselberghs, I.; Clays, K.; Persoons, A.; McDonagh, A. M.; Ward, M. D.; McCleverty, J. *Chem. Phys. Lett.* **2002**, *368*, 408.
(134) Asselberghs, I.; McDonagh, A. M.; Ward, M. D.; McCleverty, J.; Coe, B. J.; Persoons, A.; Clays, K. *SPIE Proc., Int. Soc. Opt. Eng.* **2005**, *5935*, 1.

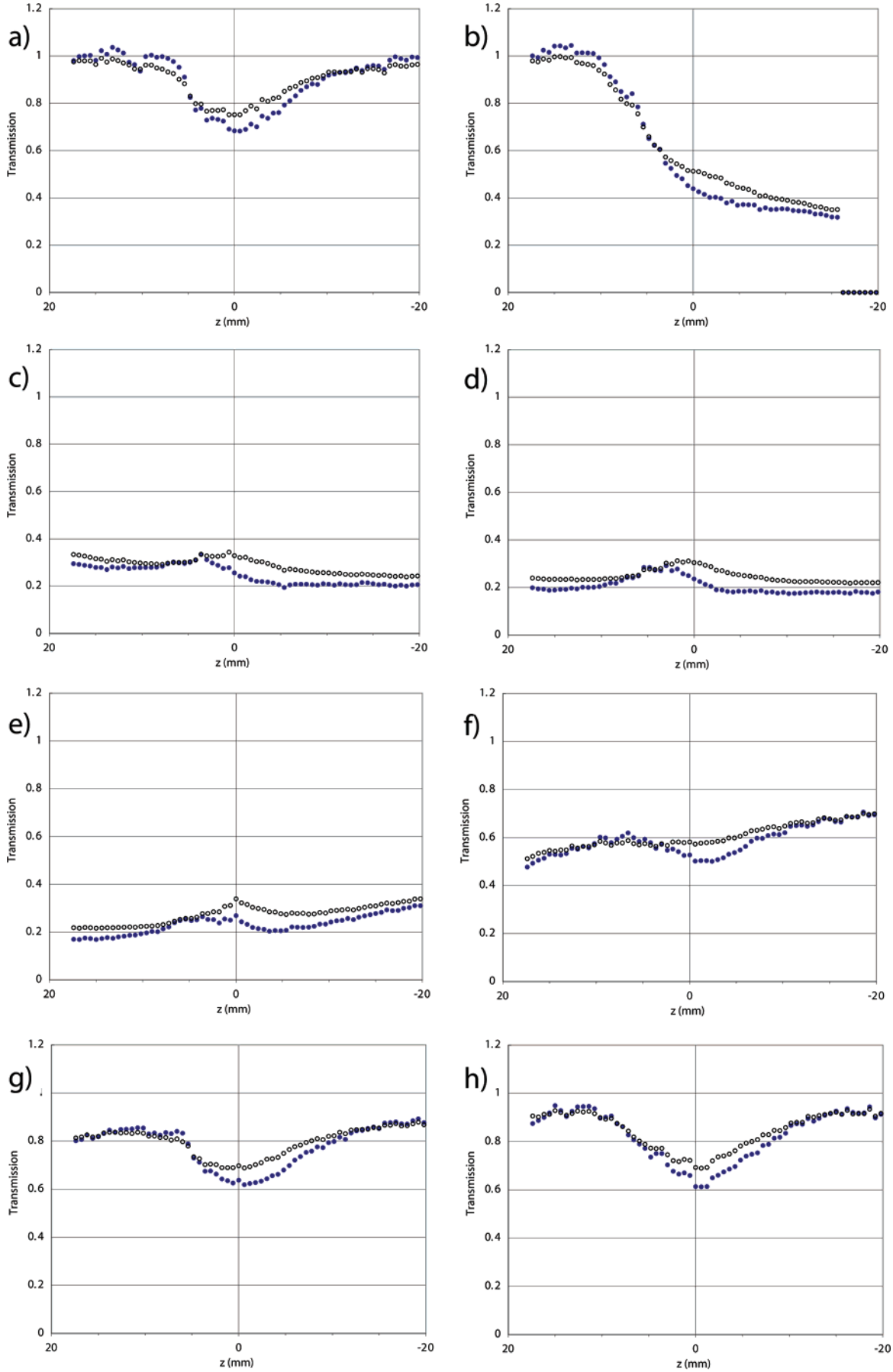

Figure 6. Change in open- (open symbols) and closed-aperture (filled symbols) Z-scan traces of **5a** over an oxidation/reduction cycle. Note that the stage traveled from positive *z* values toward negative values.

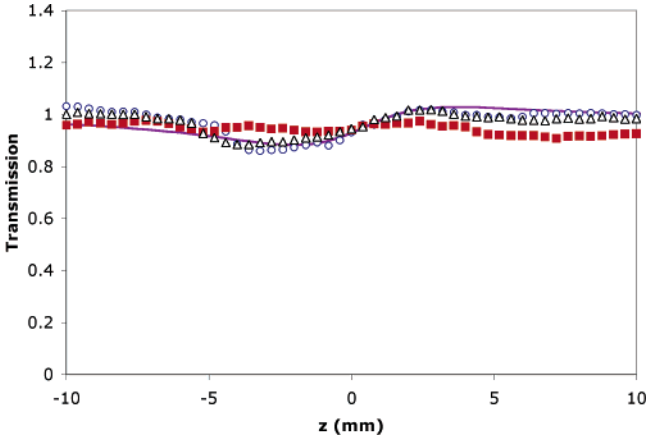

Figure 7. Closed-aperture results from the electrochromic switching of **5b** at 1180 nm.

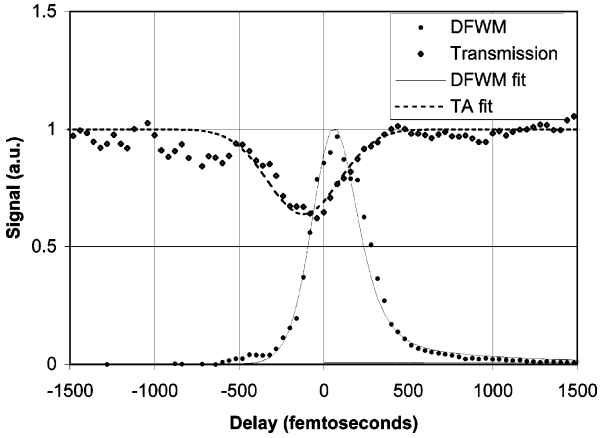

Figure 8. Simultaneous DFWM and pump−probe measurements on a solution of **5a** (0.3% w/w in CH_2Cl_2) in an electrochemical cell before oxidation.

useful. The rate of reversible electrochemical switching in the present work is diffusion controlled, and, unlike the photochromic switching, the back-reaction proceeds at essentially the same rapid rate as the forward process; very fast switching is therefore possible by electrochromic means.

Significant absorption at 12 500 cm^{-1} (corresponding to our laser irradiation wavelength of 800 nm) is seen in complex **5a** with a *trans*-[Ru(C≡CR)Cl$(L_2)_2$] (L_2 = bidentate phosphine) complex composition. This is of potential interest as most biological materials, such as tissue, have maximum transparency at this wavelength. The NIR absorption maximum of the oxidized form, and hence the frequency at which switching the absorptive nonlinearity can occur, is tunable in complexes such as these by appropriate molecular modification. Replacing the chloride with a second alkynyl ligand, to afford *trans*-[Ru(C≡CR)(C≡CR′)$(L_2)_2$], results in complexes with enhanced σ_2 (Table 3), but also results in the absorption maximum in the oxidized form of the complexes being shifted to significantly lower energy (Table 1), and with appreciable absorption at 1300 nm (7700 cm^{-1}). This is a wavelength at which silica has good transparency, affording the prospect of electrochromic switching devices at a telecommunications-relevant wavelength. This possibility was pursued with the bis-alkynyl complexes **5b** and **6a**. Results obtained at longer wavelengths can only be considered preliminary at this stage, analysis indicating that they are influenced to some degree by additional effects which may be due to nonlinearities of non-electronic, possibly thermal, origin. Overtone absorption seemed to affect our Z-scans at 1300 nm, leading to difficulties in interpreting the Z-scans for the electrochemical cell containing the electrolyte. Figure 7 shows the nonlinear electrochromic switching effect in a solution of **5b** at 1180 nm. Circles denote the closed-aperture results of the neutral species, squares show the closed-aperture results after oxidation at 0.8 V, and triangles represent the closed-aperture Z-scan results after the potential is returned to 0.0 V. The closed-aperture Z-scans indicate that the refractive nonlinearity of the solution is positive for the neutral form of **5b** but becomes close to zero for the oxidized form at the 0.8 V potential. The effect is reversible: the curve after the oxidation−reduction cycle is essentially identical to the starting curve. In contrast to results obtained at 800 nm, nonlinear absorptive effects appear to be of little significance at 1180 nm. There is no indication of an efficient two-photon absorption effect at this wavelength for the complex in the resting state, which is not surprising because this wavelength divided by 2 (590 nm) is far removed from the range of one-photon absorption. In addition, the open-aperture curve is featureless following conversion into the oxidized form, so any absorption saturation effects must be relatively weak at the measurement wavelength. Thus, the main effect which is observed at 1180 nm is the "switching off" of the large positive refractive nonlinearity of **5b** ($\gamma_{real,1180}$: **5b** 5000 × 10^{-36} esu, $\mathbf{5b}^{3+}$ < 500 × 10^{-36} esu; $\gamma_{imag,1180}$: **5b** 400 × 10^{-36} esu, $\mathbf{5b}^{3+}$ < 200 × 10^{-36} esu). This Z-scan result is tentative and should be confirmed by other experimental techniques. The usual difficulty of interpretation of Z-scan in the presence of absorption is that the refractive nonlinearity observed in such an experiment may be contaminated by the presence of a thermal component. Such a component is usually negative, due to a negative value of d*n*/d*T* for most solvents. The experiments were carried out at 1 kHz, and this higher repetition rate may exacerbate the difficulty in avoiding contributions from thermal effects.

The Z-scan measurements at 1180 and 1300 nm can only be considered qualitative at this time, and time-resolved techniques will be used in future studies to separate the electronic NLO effects from other types of nonlinearities at these wavelengths. The temporal nature of the effects giving rise to these electrochemically switchable NLO effects at the various wavelengths is clearly of interest, so to afford some insight we have interrogated one of the electrochemically switchable systems at 800 nm (12 500 cm^{-1}) (**5a**) with a combination of femtosecond time-resolved DFWM and transient absorption (TA). Typical DFWM and TA scans at 12 500 cm^{-1}, recorded on pristine samples of **5a** in the electrochemical cell, are presented in Figure 8. The DFWM curve is somewhat unsymmetrical, with a slight "tail" for positive delays; this is typical behavior when two-photon-generated excited states persist for some time after the excitation (see, e.g., ref 136). The magnitude of the DFWM signal of the **5a** solution was compared with that of a 1 mm thick piece of silica and found to be ca. 22 times greater. [Since the DFWM signal can be presented as

(135) Sekkat, Z.; Knoesen, A.; Lee, V. Y.; Miller, R. D. *J. Phys. Chem. B* **1997**, *101*, 4733.

(136) Pang, Y.; Samoc, M.; Prasad, P. N. *J. Chem. Phys.* **1991**, *94*, 5282.

$$I_{\mathrm{DFWM}} \propto \frac{(\chi^{(3)})^2}{n_0^4} L_{\mathrm{eff}}^2 I_{\mathrm{pump}}^3$$

where L_{eff} is the effective length of the interaction, the signal ratio can be used to determine $|\chi^{(3)}|$ of the solution and hence $|\gamma|$ for the solute; note, however, that one needs to account for the nonlinearity of the solvent and the electrolyte.][97] The value estimated from this comparison ($|\gamma| \approx 2000 \times 10^{-36}$ esu) is in good agreement with our Z-scan results ($(2200 \pm 600) \times 10^{-36}$ esu). The changes of transmission (a dip at the delay time close to zero) seen in the pump−probe signal in Figure 8 are consistent with the Z-scan results, indicating efficient two-photon absorption in **5a**. The depth of the dip can be interpreted as $\Delta T = 1 - \exp(-\beta_2 I_{\mathrm{pump}} L_{\mathrm{eff}})$, affording the two-photon absorption coefficient $\beta_2 = 0.05$ cm GW^{-1} for the 0.3% w/w solution and leading to $\sigma_2 \approx 10^{-47}$ cm^4 s (10^3 GM units), again in reasonable agreement with $\sigma_2 = 0.53 \times 10^{-47}$ cm^4 s determined by the Z-scan studies of γ_{imag}.

Oxidation and reduction cycles in the electrochemical cell were then carried out, monitoring both the transmission signal and the DFWM signal. Oxidation of the 0.3% w/w solution of **5a** to **5a**$^{3+}$ caused the transmission (T) at 800 nm to decrease to about 10% of that before oxidation, while the DFWM signal decreased by a smaller amount. The changes of this signal should be interpreted taking into account an absorption correction for the effective interaction length. This leads to the following expression for the changes of the DFWM signal:

$$\frac{I_{\mathrm{DFWM,oxidized}}}{I_{\mathrm{DFWM,neutral}}} = \left(\frac{|n_2|_{\mathrm{oxidized}}}{|n_2|_{\mathrm{neutral}}} \frac{(T-1)\sqrt{T}}{\ln(T)} \right)^2$$

Introducing corrections for the transmission changes, one finds that the modulus of the nonlinearity of the solution actually increases on oxidation, as shown in Figure 9.

Figure 10 shows the time-resolved signals obtained for a solution of **5a**$^{3+}$ after the oxidation was completed. Two major differences are seen compared to the signals in Figure 8: the DFWM signal is now dominated by a delayed response, with a characteristic time of about 1 ps, and the TA signal is now positive (indicating absorption saturation effects), with a decay time that is also of the order of 1 ps (the apparent difference in the decay rate seen in the figure is the result of the fact that the solution extinction depends linearly on the time-dependent concentration of transient absorbing species while the DFWM signal depends on the square of this concentration). Taking into account a suitable absorption correction, the magnitude of the DFWM signal after oxidation affords a value of ca. 20×10^{-33} esu for $|\gamma|$ of **5a**$^{3+}$, about 10 times larger than that for the neutral molecule, and once again in good agreement with the Z-scan result ($(14\,000 \pm 3000) \times 10^{-36}$ esu). The change in the character of the TA signal also confirms the change of sign of γ_{imag}.

Discussion. The π-delocalizable linear, octupolar, and dendritic alkynylruthenium complexes in the present study comprise a systematically varied suite of compounds for which electron richness of the metal center (as assessed by cyclic voltammetry) and linear optical behavior (from UV−vis−NIR spectroscopy) can be tuned in a rational fashion by ligand modification. While the presence of one oxidation wave for the polymetallic complexes is consistent with non-interacting metal centers,

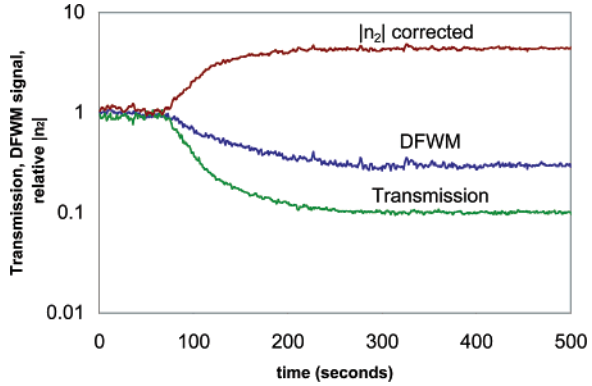

Figure 9. Changes of transmission, the peak DFWM signal, and the absorption-corrected solution nonlinearity as a function of time on oxidizing a 0.3% w/w solution of **5a** in CH_2Cl_2.

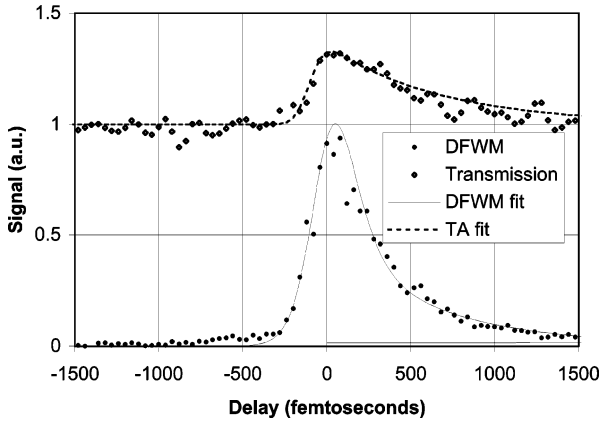

Figure 10. Simultaneous DFWM and pump−probe measurements on a solution of **5a**$^{3+}$ (0.3% w/w in CH_2Cl_2) in an electrochemical cell after oxidation.

progression from **7a**,**b**,**d** to **5a**,**b**,**d** results in a red-shift in ν_{max}, suggestive of an increase in π-delocalization on proceeding from a linear to a trigonally branched complex. Although a slight red-shift in ν_{max} is observed on progressing from zero-generation dendrimer **5c** to the first-generation example **6b**, a blue-shift is seen on proceeding from **5b** to **6a** that, coupled to HRS depolarization studies, suggests onset of a lack of coplanarity upon π-extension through the metal and progression to the dendrimer. Quadratic nonlinearities increase dramatically on introduction of peripheral nitro substituents and, indeed, for **6b** are very large for a formally octupolar molecule, but the suspicion exists that a D_{3h} idealized geometry does not exist for these complexes in solution; the EA data are consistent with a strongly dipolar charge-transfer contribution to quadratic nonlinearity, probably a dendritic arm-localized charge transfer, and are inconsistent with octupolar and global charge transfer.

Both real and imaginary components of the cubic nonlinearities of these dendrimers are significant, the TPA cross sections in particular being very large. Our attempt to quantify the increase on proceeding from linear to octupolar and then dendritic complexes (proceeding from **7b** to **5b** to **6a**) is tantalizing and suggestive of a "dendritic effect" that must be confirmed by a complete wavelength dependence study. The large nonlinearities indicate potential in optical limiting; pump−probe studies at 527 nm, however, are consistent with an absorption saturation effect for which the excited-state lifetime increases on proceeding to the dendrimer.

These large TPA cross sections are noteworthy but are similar in magnitude to those of the best organic compounds. One area in which organometallic complexes may be superior to organic molecules is the electrochemically induced switching of NLO properties, because of the presence of readily accessible reversible redox processes at metal centers. For the present complexes, ligand variation can be used to tune the crucial region of nonlinear electrochromism between 800 nm (corresponding to maximum transparency in tissue, and therefore of biological interest in, for example, imaging) and 1180−1300 nm (the latter corresponding to maximum transparency in silica, and therefore of interest in telecommunications). Switching of both refractive and absorptive nonlinearity has been demonstrated in the present studies; at short wavelength, oxidation corresponds to a change from self-defocusing to self-focusing behavior and from a two-photon absorber to a saturable absorber, and at long wavelength, oxidation results in the loss of self-focusing behavior. Organic compounds with enhanced NLO properties have been intensively scrutinized in an effort to develop materials to control and process signal-carrying light beams, of enormous current interest in photonics. The present work adds a new dimension to this area: the electrochemical switching of nonlinear refraction and nonlinear absorption are higher order (or nonlinear) electrochromic effects that have been shown to originate in picosecond time scale processes in these electron-rich organometallic dendrimers by a combination of Z-scan, DFWM, and pump−probe studies.

Acknowledgment. We thank the Australian Research Council, the Fund for Scientific Research-Flanders (G.0338.98, G.0407.98 and G.0297.04), the Belgium Government (IUAP-IV/11 and IUA-V/3), the K.U. Leuven (GOA/2000/03 and GOA/2006/03), and the Japan Science and Technology Corporation (Core Research for Evolutional Science and Technology program "Hyper-Structured Molecules and Their Application to Organic Quantum Devices" project headed by Prof. H. Sasabe, Chitose Institute of Science and Technology, Japan) for support of this work, and Johnson-Matthey Technology Centre for the generous loan of ruthenium salts. M.G.H. is an ARC Australian Professorial Fellow, M.P.C. is an ARC Australian Research Fellow, and A.M.M. and N.T.L. held Australian Postgraduate Awards. M.G.H. thanks the Science and Technology Agency of Japan (STA) for a Fellowship.

JA062246V